Synthesis, magnetic, spectral and antimicrobial studies on metal complexes of 4-methylphenylaminoacetoisatin hydrazone

Abdou Saad El-Tabl*, Ramadan Mahdy El-Bahnasawy and Alaa El-Deen Hamdy

Chemistry Department, Faculty of Science, Menuofia University, Shebin El -Kom, Egypt

A new series of Mn(II), Co(II), Ni(II), Cu(II), Zn(II), Cd(II), Cr(III), Fe(III) and Cu(I) complexes of 4-methylphenyl-aminoacetoisatin hydrazone (HL) have been prepared and characterised The IR spectral data of the complexes indicate neutral bidentate, neutral tridentate or monobasic tridentate behaviour of the ligand depending on the metal ion. The ESR spectra of the complexes [Cu(OAc) (L)].0.5H$_2$O, [CuCl(L)].0.5H$_2$O, [Cr(Cl)(OH)$_2$(HL)].0.5H$_2$O, Co(NO$_3$)$_2$[(HL)$_2$].2.5H$_2$O and [(HL)(Mn)$_3$(Cl)$_4$(OH)$_2$(H$_2$O)$_6$].H$_2$O, are isotropic. However, those of [Cu(NO$_3$)(L)].2.5H$_2$O and [Cu(SO$_4$)(H$_2$O)(HL)], are anisotropic with ionic bond characters. The antibacterial and antifungal activities of the compounds show that some metal complexes exhibit a greater inhibitory effect than tetracycline (bacteria) and amphotricine (fungi).

Isatin hydrazones of metal complexes have potential activity as antitumor agents evaluated on human leukaemic cells,[1] and also exhibit anticonvulsant[2] and antibacterial activities.[3] Much work on metal complexes of isatin isonicotinoyl hydrazone has been reported.[4] However, little research has been done on metal complexes of the hydrazone derived from substituted phenyl amino acetohydrazide and isatin, so we have prepared and spectrally characterised a new hydrazone derived from 4-methylpheylaminoacetohydrazide and isatin and its metal complexes.

Experimental

Reagent grade chemicals were used, 4-methylphenylamino-acetohydrazide was prepared by a published method.[5] Elemental analyses (C, H, N and Cl) were determined by the Analytical Unit of Mansoura University, Egypt. Standard methods were used to determine the metal ion content.[6] All metal complexes were dried in a vacuum over anhydrous P$_4$O$_{10}$. The IR spectra were recorded on a Perkin-Elmer IR spectrometer 681 (4000–200 cm^{-1}), using KBr discs. Electronic spectra in DMF solutions were recorded on a Perkin-Elmer 550 spectrophotometer using 1-cm quartz cells. The molar conductances of complexes in DMF (10^{-3} M) were measured using a tip cell and a Bibby conductimeter MCl at room temperature. The ^{1}H NMR spectra of the ligand, [HL], (1) and its zinc(II), copper(I) and cadmium(II) complexes were measured in DMSO–d$_6$ as a solvent using a 300 MHZ Varian NMR spectrometer. The thermal analyses (DTA and TGA) were carried out in air on a Shimadzu DT-30 thermal analyser from 25 to 800 °C at a heating rate of 10 °C /min. The solid ESR spectra of the complexes were recorded on an ELEXSYS E500 Bruker spectrometer in 3 mm Pyrex tubes at 298 K. 1, 1-diphenyl-picrylhydrazal (DPPH) was used as a g-marker for the calibration of the spectra. Mass spectra were recorded using a JEOL JM-S-AX-500 mass spectrometer. The magnetic moments of the complexes were measured in a borosilicate tube with a Johnson Mathey magnetic susceptibility balance at room temperature, by the modified Gouy method using the equation $\mu_{eff} = 2.84(\chi_n \times T)^{1/2}$. T.L.C measurements confirmed the purity of the prepared compounds.

Preparation of the ligand and its metal complexes
Ligand [HL] (1): A hot ethanolic solution (50 cm^3) containing (6.4 g 1.0 mol) of 4-methyl phenylaminoacetohydrazide was added to a hot ethanolic solution (50 cm^3) containing (4.5 g 1.0 mol) of isatin. The mixture was refluxed on a water bath for 2 h. The product was collected at room temperature, washed several times with ethanol and dried over P$_4$O$_{10}$.

Complexes (2)–(8) and (11)–(24) were prepared by mixing stoichiometric ratios:(1 : 1), (2 : 1), or (1 : 3) of (1) (in 30 cm^3 EtOH) with the appropriate metal(I), metal(II) or metal(III) salt (chloride, acetate, nitrate, chloride or sulfate) in EtOH (50 cm^3) in the presence of triethylamine. The mixture was refluxed for 1–3 h and the resulting precipitate was filtered off, washed several times with ethanol and dried over P$_4$O$_{10}$.

Complexes (9) and (10) were prepared by mixing stoichiometric ratios (1:l) of the complexes (7) and (8) (in 30 cm^3 EtOH) with the appropriate ratios of acetylacetone (in 50 cm^3 EtOH) in the presence of triethylamine. The mixture was refluxed for 3 h and the resulting precipitate was filtered off, washed several times with ethanol and dried over P$_4$O$_{10}$.

Bacteria media
Nutrient agar medium was prepared by standard method.[5] The antibacterial activity of (1) and its complexes were tested using the paper disc diffusion method[7] against positive gram bacteria (*Staphylococcus aureus*) and gram negative bacteria (*Escherichia coli*), The tested compounds in measured quantities were dissolved in DMF to a concentration of 1000 ppm of compounds. Nutrient Agar media was poured in each Petri dish. After solidification, 0.1 cm^3 of the tested bacteria was spread over the medium using a spreader. Discs of Whatman no.1 filter paper having diameter of 5.00 mm, containing compounds were placed in the inoculated Petri plates. The plates were incubated at 28 °C for 24–48 h and the zone of inhibition was calculated in millimetres.

Fungus media
The tested compounds in measured quantities were dissolved in DMF to a concentration of 1000 ppm of compounds. Czapek dox agar medium was prepared by a standard method.[5] *Aspergillus flavus* or *Cadida albicans* was spread over each dish by using a sterile bent loop rod. Disks were cut by a sterilised cork borer and then taken by sterilised needle. The resulting pits were sites for the test compounds, the plates are sites for the tested compounds. The plates were incubated at 30 °C for 24–48 h and any clear zones present were detected, the zone of inhibition was calculated in millimetres.

Results and discussion

The reaction of 4-methylphenylaminoacetohydrazide with isatin in EtOH (1:1, molar ratio), gave [HL], (1) as shown in Scheme 1. All complexes are intensely coloured, crystalline solids and stable at room temperature and not decomposing after prolonged storage. They are insoluble in non-polar and polar solvents but soluble in polar coordinating solvents such as DMSO and DMF. Elemental analyses and physical data (Table 1), and spectral data (Tables 2 and 3†)
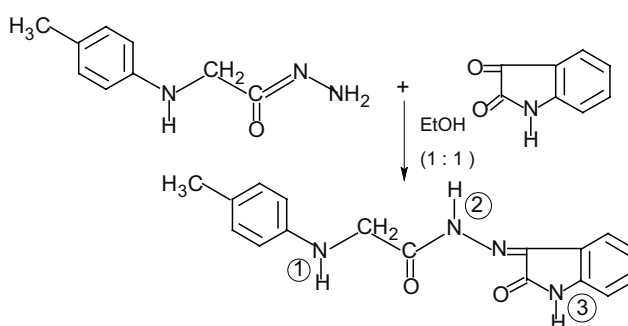
Scheme 1

* Correspondent. E-mail: asaeltabl@yahoo.com

Table 1 The elemental analyses of the ligand [HL] and its metal complexes

No.	Compound/complex	Mol.wt.	Colour	M. p./°C	A^a_M	Yield /%	$\mu_{eff.}$	Calcd (Found%)				
								C	H	N	M	Cl
1	[HL]$C_{17}H_{16}N_4O_2$	308.31	Orange	248	—	80	–	66.22 (65.72)	5.23 (5.13)	18.16 (18.21)	–	–
2	[(L)Cu(OAc)].1/2H_2O($C_{19}H_{19}N_4O_{4.5}$Cu)	438.91	Black	>300	12.0	70	1.84	51.99 (52.55)	4.36 (4.37)	12.75 (12.26)	14.47 (14.00)	–
3	[(L)Co(OAc)].H_2O($C_{19}H_{20}N_4O_5$Co)	443.30	Brown	>300	19.0	65	3.48	51.47 (50.85)	4.54 (4.49)	12.63 (12.38)	13.29 (12.98)	–
4	[(L)Ni(OAc)].2H_2O($C_{19}H_{22}N_4O_6$Ni)	461.07	Yellow	>300	14.6	60	Dia.	49.49 (49.09)	4.80 (3.23)	12.14 (12.00)	12.73 (12.21)	–
5	[(L)Zn(OAc)].2H_2O($C_{19}H_{22}N_4O_6$Zn)	465.76	Brown	>300	18.9	64	Dia.	48.99 (48.29)	4.76 (5.41)	12.02 (11.22)	13.60 (13.12)	–
6	[(L)Cd(OAc)]($C_{19}H_{18}N_4O_4$Cd)	478.75	D. Brown	>300	5.4	56	Dia.	47.67 (48.18)	3.79 (3.54)	11.69 (11.21)	23.48 (23.15)	–
7	[(L)Mn$_2$(OAc)$_3$(H_2O)$_4$].6H_2O($C_{23}H_{44}N_4O_{18}Mn_2$)	774.48	Red	>300	20.0	71	2.82	35.66 (34.44)	5.72 (5.32)	7.23 (6.51)	14.28 (13.50)	–
8	[(L)Ni$_2$(OAc)$_3$(H_2O)$_4$].6H_2O($C_{23}H_{44}N_4O_{18}Ni_2$)	782.00	Brown	>300	19.5	64	2.13	35.32 (34.20)	5.67 (5.32)	7.16 (6.32)	15.00 (14.47)	–
9	[(L)Mn(acac)(H_2O)].3H_2O($C_{22}H_{30}N_4O_8Mn$)	533.42	Brown	>300	17.0	67	6.84	49.53 (49.08)	5.66 (5.27)	10.49 (10.51)	10.29 (10.32)	–
10	[(L)Ni(acac)(OAc)].3H_2O($C_{24}H_{31}N_4O_9Ni$)	578.21	Brown	>300	4.7	50	2.95	49.85 (50.04)	5.40 (5.91)	9.68 (9.64)	10.15 (10.12)	–
11	[(L)Cu(NO$_3$)].2.5H_2O($C_{17}H_{20}N_5O_{7.5}$Cu)	477.89	Brown	>300	23.0	68	1.79	42.72 (42.28)	4.21 (5.39)	14.64 (14.01)	13.29 (12.85)	–
12	[(L)Ni(NO$_3$)].H_2O($C_{17}H_{17}N_5O_6$Ni)	446.02	Black	>300	1.90	61	Dia.	45.77 (45.23)	3.84 (4.04)	15.69 (15.96)	13.16 (13.41)	–
13	[(HL)$_2$Co(NO$_3$)$_2$].2.5H_2O($C_{34}H_{37}N_{10}O_{12.5}$Co)	844.60	D. Brown	>300	18.1	55	3.85	48.35 (48.61)	4.41 (4.03)	16.57 (16.60)	6.97 (6.85)	–
14	[(HL)$_2$Zn(NO$_3$)$_2$].H_2O($C_{34}H_{34}N_{10}O_{11}$Zn)	822.02	Black	>300	16.4	60	Dia.	49.67 (50.18)	4.16 (4.21)	17.03 (17.21)	7.71 (7.82)	–
15	[(HL)$_2$Cd(NO$_3$)$_2$]($C_{34}H_{32}N_{10}O_{10}$Cd)	853.03	D. Red	>300	15.0	60	Dia.	47.87 (47.32)	3.78 (3.96)	16.41 (16.21)	13.17 (12.86)	–
16	[(L)CuCl].1/2H_2O($C_{17}H_{16}N_4O_{2.5}$ClCu)	415.31	Brown	>300	19.4	61	1.80	49.16 (48.85)	3.88 (4.19)	13.48 (13.41)	15.30 (15.21)	8.53 (8.60)
17	[(L)NiCl].4.5H_2O($C_{17}H_{24}N_4O_{6.5}$ClNi)	482.52	Yellow	>300	5.1	59	Dia.	42.31 (42.13)	5.01 (5.75)	11.60 (11.50)	12.16 (12.31)	7.34 (7.40)
18	[(L)ZnCl].2.5H_2O($C_{17}H_{20}N_4O_{4.5}$ClZn)	451.17	Brown	>300	17	61	Dia.	45.25 (45.41)	4.46 (5.34)	12.41 (12.20)	14.04 (13.90)	7.85 (7.41)
19	[(HL)Co$_2$(Cl)$_2$(OH)$_2$(H_2O)$_4$].H_2O ($C_{17}H_{28}N_4O_9Cl_2Co_2$)	621.13	Brown	>300	15.3	64	2.81	32.87 (32.91)	4.54 (4.21)	9.01 (8.92)	18.97 (19.08)	11.41 (11.66)
20	[(HL)Fe(Cl)$_2$(OH) (H_2O)].5H_2O($C_{17}H_{29}N_4O_9Cl_2$Fe)	560.15	Black	>300	14.0	67	5.61	36.45 (36.88)	5.21 (5.77)	9.99 (9.98)	9.96 (9.32)	12.65 (12.11)
21	[(HL)Cr(Cl)(OH)$_2$].1/2H_2O($C_{17}H_{19}N_4O_{4.5}$Cl$_2$Cr)	438.78	Brown	>300	11.9	72	3.44	46.53 (46.89)	4.36 (4.70)	12.75 (12.12)	11.85 (11.30)	8.09 (7.80)
22	[(HL)$_2$Cu$_2$Cl$_2$].1.5H_2O($C_{34}H_{35}N_8O_{5.5}$Cl$_2$Cu$_2$)	841.55	Y. brown	>300	21.0	69	Dia.	48.52 (48.21)	4.19 (4.25)	13.30 (13.46)	15.09 (14.91)	8.42 (8.71)
23	[(HL)Cu(SO$_4$)H_2O]($C_{17}H_{18}N_4O_7$SCu)	485.93	Brown	>300	11.0	70	1.70	42.02 (42.32)	3.73 (4.13)	11.52 (11.16)	13.07 (13.41)	–
24	[(HL)(Mn)$_3$(Cl)$_4$(OH)$_2$(H_2O)$_6$].H_2O ($C_{17}H_{32}N_4O_{11}Cl_4Mn_3$)	775.06	Brown	>300	23.40	58	3.70	26.34 (26.58)	4.16 (3.98)	7.22 (7.13)	21.26 (20.94)	18.29 (18.11)

$A^a_{M=}$ molar conductivity, D. = dark, Y. = yellowish, acac = acetylacetone

are compatible with the proposed structures (Fig. 1). To date, no diffractable crystals have been grown.

Conductivity measurements
The molar conductance values of the complexes in DMF (10^{-3} M) lie in the (1.90–23.40 Ω^{-1} cm^2 mol^{-1}) range (Table 1). The low values indicate that all the complexes are non electrolytes.[8] This confirms that the anion is coordinated to the metal ion.

^{1}H NMR of the (1) and some metal complexes
The ^{1}H NMR spectrum of (1) in DMSO-d$_6$ confirms the proposed structure (Fig. 1). The spectrum shows two peaks for the NH group at 11.12, 10.81 ppm and another peak for the OH group at 13.54 ppm.[9] The integration of the two sets of signals related to NH and OH groups gives the ratio 50:25, this is evidence for the presence of enol and keto-forms of the ligand as shown in Scheme 2.
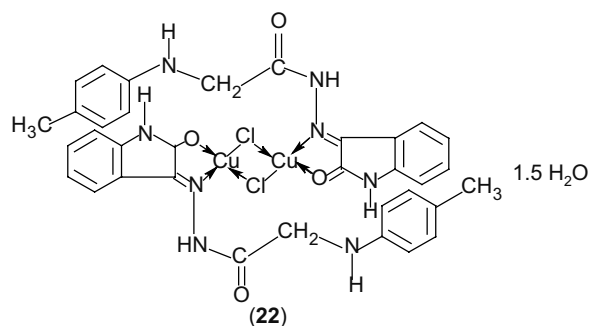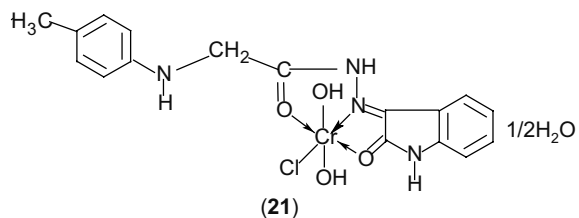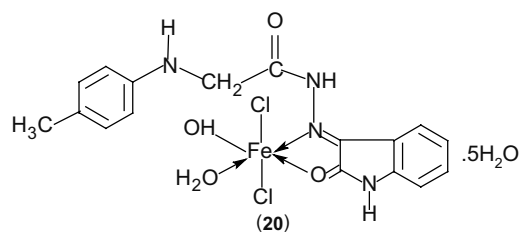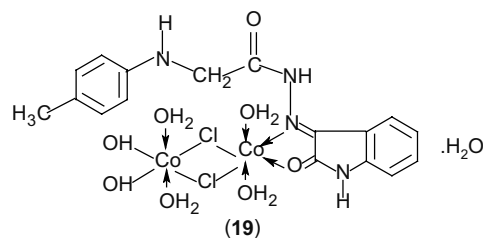

Scheme 2

Fig. 1

(**23**)

(**24**)
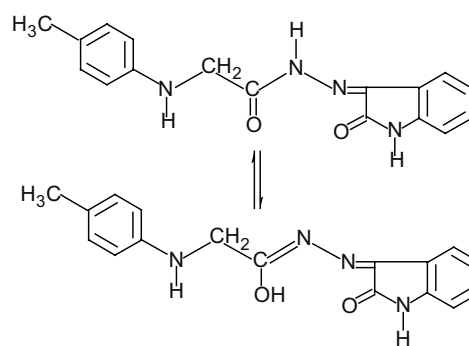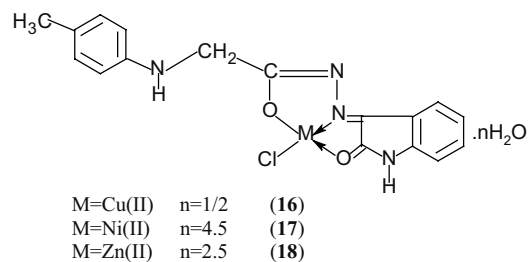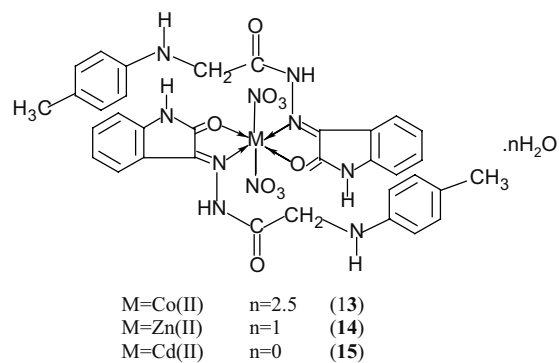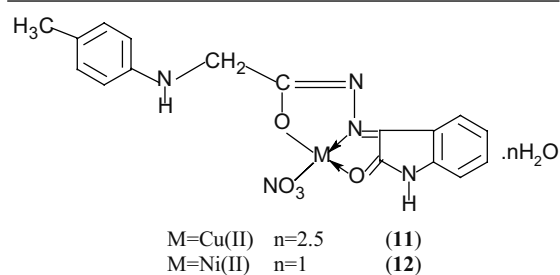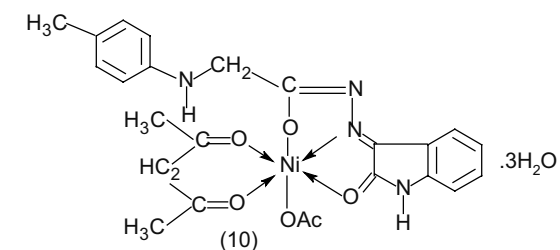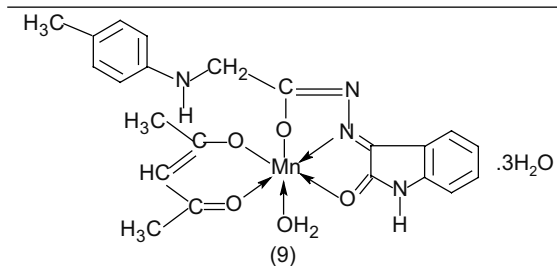
Fig. 1 *Continued*

The peaks in the 6.20–7.39 ppm range are assigned to the protons of the aromatic ring and the singlet peaks at 3.35 and 4.34 ppm, to protons of methyl and methylene groups respectively.[5] Zinc(II) complex (**14**) shows multiplet peaks in the 6.55–7.53 ppm range, assigned to the aromatic protons and the NH group appears at 7.69 ppm. The peaks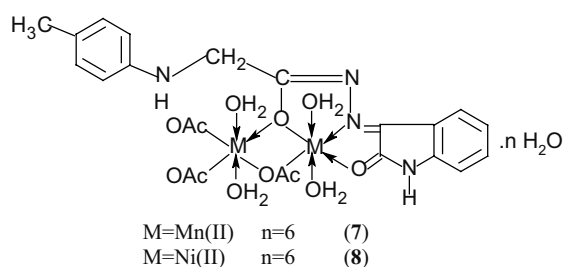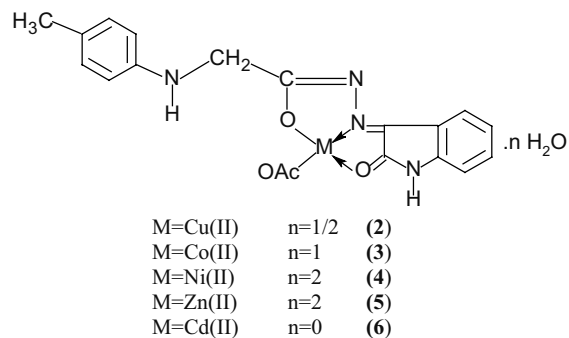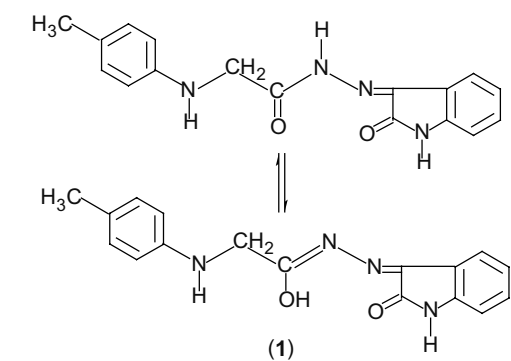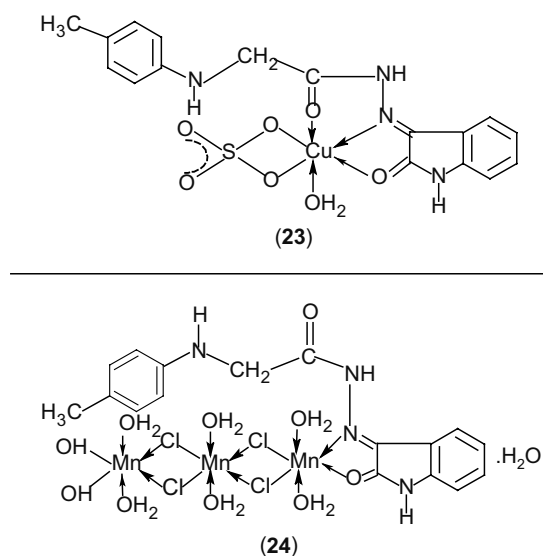 at 3.34 and 4.24 ppm, are due to the protons of methyl and methylene groups respectively.[5] The zinc(II) complex (**18**) shows aromatic protons as multiplet peaks in the 6.60–6.93 ppm range, and peaks at 3.40 and 4.25 ppm due to the protons of methyl and methylene groups respectively.[5] The signal due to NH proton had disappeared, confirming the proposed structure. The cadmium(II) complex (**15**) shows aromatic proton resonances in the 6.64-6.90 ppm range, the NH proton at 7.69 ppm. and the protons of methyl and methylene groups respectively[5] at 3.33 and 4.26 ppm, The copper(I) complex (**22**) shows aromatic protons in the 6.94–7.29 ppm range, the NH proton at 7.70 ppm. and the protons of methyl and methylene groups at 3.34 and 4.22 ppm respectively.[5] The ^{1}H NMR spectra of the ligand and its Zn(II) complex are shown in Fig. 2[†].

Mass spectrum of the ligand, (1)
The mass spectrum of the ligand reveals the molecular ion peak (*m/z*) at 308 a.m.u. consistent with the molecular weight. and the fragments at *m/z* = 78, 91, 106, 120, 145, 148 and 163 corresponding to $C_6H_6^+$, $C_7H_7^+$, $C_7H_8N^+$, $C_8H_{10}N^+$, $C_8H_5N_2O^+$, $C_9H_{10}NO^+$ and $C_9H_{11}N_2O^+$ respectively, (Table 4[†]). The suggested mechanism of the fragmentation of the ligand is shown in Fig. 3[†].

IR spectra
Important spectral bands of (**1**) and its metal complexes are presented in Table 2[†]. The IR spectrum of (**1**) shows broad strong bands in 3550–3320 and 3300–2820 cm^{-1} ranges, which are attributed to intra- and intermolecular hydrogen bonding of OH groupings.[10] Also, the spectrum shows $\nu(NH)_{(1), s, as}$ at 3420 and 1522, $\nu(NH)_{(2), s, as}$ at 3387 and 1462, $\nu(NH)_{(3), s, as}$ at 3238 and 1458 cm^{-1} respectively.[11] Other bands at 1720, 1702 and 1618 cm^{-1} are assigned to the $\nu(C=O)$ hydrazide, $\nu(C=O)$ring and $\nu(C=N)$ respectively.[11-13] Strong bands appear in the 1590–1522 cm^{-1} range and at 1369 cm^{-1}, corresponding to $\nu(C=C)_{Ar}$ and $\nu(C–O)$ respectively.[12,14]

Comparison of the spectra of the complexes with that of (**1**) shows shifts of characteristic bands. Bands observed in the ranges 3421–3417, 1531–1514, 3385–3381, 1460–1455, 3223–3205 and 1466–1452 cm^{-1} are due to $\nu(NH)_{(1)}$, $\nu(NH)_{(2)}$ and $\nu(NH)_{(3)}$ respectively[13] (Table 2[†]). The complexes show bands in the 1727–1650 and 1644–1591 cm^{-1} ranges assignable to $\nu(C=O)$ and $\nu(C=N)$ respectively. The shift of the band due to $\nu(C=O)$ in the 9–52 cm^{-1} range indicates a minor change in symmetry of this group due to metal coordination. Also, the shift of $\nu(C=N)$ in the 6–27 cm^{-1} range is evidence for the coordination of the azomethine nitrogen atom to the metal ions.[15] Broad bands were observed in the 3660–3190 and 3470–3125 cm^{-1} ranges which are assigned to $\nu(OH)$ of hydrated water [except for (**6**), (**15**) and (**23**)] or coordinated water molecules [except (**2**)–(**6**), (**10**)–(**18**), (**21**) and (**22**)].[14,16]

The complexes show broad bands in the 3570–3115 and 3270–2650 cm^{-1} ranges indicating intra- and intermolecular hydrogen bondings in the complexes.[11] Complexes (**2**)-(**8**) and (**10**) show two bands in the 1589–1523 and 1405–1326 cm^{-1} ranges, due to $\nu(C=O)$ and $\nu(C–O)$ of the acetate group. The difference between these bands (in the 236–155 cm^{-1} range), enable us to suggest that the acetate group is coordinated to the metal ions in a unidentate fashion.[17] However, complexes (**7**) and (**8**) show bands at 1558, 1416, and 1560, 1417 cm^{-1}; the difference between these bands is equal to 142 and 143 cm^{-1} respectively, indicating bridging acetate.[18] Complexes (**2**)–(**12**) and (**16**)–(**18**) show bands in the 1280–1298 cm^{-1} range, assigned to (C–O), the shift of this band by 7–89 cm^{-1} compared to that of the ligand, indicates coordination of this group to the metal ion. Complexes (**11**)–(**15**) show four bands in the 1386–1377, 1290–1103, 850–789 and 751–740 cm^{-1} ranges, which are assigned to a terminal nitrate group.[19] Complexes (**16**)–(**22**) show band in the 460–379 cm^{-1} range, due to the coordination of chloride.[19] Complex (**23**) shows strong bands at 1201, 1121, 1025 and 977 cm^{-1}, due to bidentate, coordinated sulfate.[11,20] Complexes (**20**), (**21**) and (**24**) show $\nu(OH)$ at 1074, 1070 and 1098 cm^{-1}.[11] The bonding of (**1**) to the metal ions through the oxygen and nitrogen atoms is supported by the presence of new bands in the 680–558 and 553–467 cm^{-1} ranges, due to $\nu(M–O)$ and $\nu(M–N)$ respectively.[21,22]

Magnetic moments
The room temperature magnetic moments of the complexes (**2**)–(**24**) are shown in Table 1. Nickel(II) complexes (**4**), (**12**) and (**17**) are diamagnetic, indicating square planar geometry, however, complexes (**8**) and (**10**) show values 2.13 and 2.95 B.M., indicating an octahedral structure.[20,23-25] The low value of complex (**8**) indicates spin-exchange interactions taking place between the nickel(II) ions. The cobalt(II) complexes (**3**), (**13**) and (**19**) show the values 3.48, 3.85 and 2.81 B.M. respectively, indicating high- spin square planar or octahedral cobalt(II) complexes.[5,9,26] The low value of complex (**19**), suggests spin-exchange interactions taking place between the cobalt(II) ions. The manganese(II) complexes (**7**), (**9**) and (**24**) show values 2.82, 6.84 and 3.70 B.M. respectively, indicating high-spin octahedral manganese(II) complexes.[9] The low values of complexes (**7**) and (**24**), indicate spin-exchange interactions taking place between the manganese(II) ions. Copper(II) complexes (**2**), (**11**), (**16**) and (**23**) show values 1.84, 1.79, 1.80 and 1.70 B.M. respectively, which corresponding to one unpaired electron in a square planar or octahedral structure.[9] Iron(III) complex (**20**) has a value 5.61 B.M. indicating a high-spin octahedral iron(III) complex.[27] Chromium(III) complex (**21**) shows a value of 3.44 B.M, which indicates an octahedral chromium(III) complex.[28] However, zinc(II) complexes (**5**), (**14**) and (**18**), cadmium(II) complexes (**6**) and (**15**) and the copper(I) complex (**22**) are diamagnetic as expected.

ESR spectra
The ESR spectra of solid copper(II) complexes (**2**) and (**16**) at room temperature are characteristic of species with the d[9] configuration and the isotropic type of resonance, (g_{iso} = 2.15 and 2.10 respectively), indicates octahedral or square planar geometry around the copper(II) ion.[5,29] Copper(II) complexes (**11**) and (**23**) in polycrystalline state at room temperature exhibit anisotropic signals with two g values, $g_\parallel$ = 2.33, 2.35 and $g\perp$ = 2.06, 2.063 with g_{iso} = 2.15 and 2.16 respectively. The $g_\parallel > g\perp > g_e$ observation suggests a tetragonal distortion around the copper(II) ions, corresponding to elongation along the fourfold symmetry z-axis with a $d_{(x2-y2)}$ ground state.[30,31] In addition, exchange coupling interactions between two copper(II) ions is explained by the Hathaway expression[32] G = ($g_\parallel$-2)/($g\perp$-2). If the value G >4.0, the exchange interaction is negligible, which is the case for complexes (**11**) and (**23**), (G = 5.50, 5.55 respectively).[30,31] Also, the $g_\parallel$ value in the copper(II) complexes can be used as a measure of the covalent character of the metal–ligand bond. If this value is greater than 2.3, the environment is essentially ionic and values less than this limit indicate a covalent environment. The $g_\parallel$-values for complexes (**11**) and (**23**) indicate ionic bond character.[29] The ESR spectrum of chromium(III) complex (**21**) shows isotropic-type symmetry with g_{iso} = 2.26, typical of chromium(III) octahedral geometry.[5] Cobalt(II) complex (**13**) has an isotropic-type resonance with g_{iso} = 2.06, indicating an octahedral cobalt(II) ion.[5,31] and the manganese(II) complex (**24**) shows an isotropic type symmetry with g_{iso} = 2.004, typical of manganese octahedral geometry.[23] The cobalt(II) complex (**3**) at room temperature do not show ESR signal because the rapid spin lattice relaxation of the cobalt(II) broadness the lines at room temperature.[33] The ESR spectrum of manganese(II)
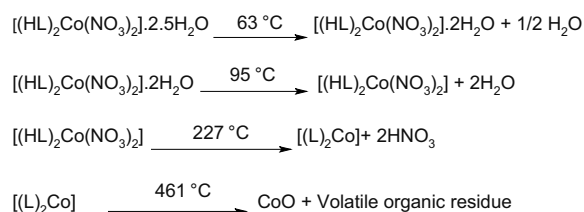
complex (**24**) is shown in Fig. 4†. The ESR parameters for the complexes are shown in Table 5†.

Electronic spectra

The electronic spectral data for the ligand and its metal complexes are summarised in Table 3†. The ligand in DMF solution shows three bands at 275 nm ($\varepsilon = 0.46 \times 10^3$ mol^{-1}cm^{-1}), 345 nm ($\varepsilon = 1.40 \times 10^3$ mol^{-1}cm^{-1}) and 355 nm ($\varepsilon = 1.36 \times 1$ 0^3 mol^{-1}cm^{-1}). The first band may be assigned to an intraligand $\pi \rightarrow \pi^*$ transition which is nearly unchanged on complexation, whereas the second and third bands may be assigned to the n$\rightarrow\pi^*$ and charge transfer transitions of the azomethine and carbonyl groups respectively.[34] These bands are shifted on complexation, suggesting the coordination of the azomethine nitrogen atom and carbonyl group to the metal ion. Nickel(II) complexes (**8**) and (**10**) show three bands in the 475–482, 620–625 and 845–870 nm ranges, which are attributable to $^3A_{2g}(F)\rightarrow^3T_{1g}(P)(\nu_3)$, $^3A_{2g}(F)\rightarrow^3T_{1g}(F)(\nu_2)$ and $^3A_{2g}(F)\rightarrow^3T_{2g}(F)(\nu_1)$ transitions respectively, of octahedral nickel(II) complexes.[9,35,36] The ν_2/ν_1 ratio for the complexes (**8**) and (**10**) are 1.40 and 1.35 (Table 3†), which are less than the usual range of 1.50–1.75, indicating distorted octahedral nickel(II) complexes.[37] Complexes (**4**), (**12**) and (**17**) show the first band in the 540–550 nm range, which is assigned to the $^1A_{2g}\leftarrow^1A_{1g}$ transition ($b_{2g}\rightarrow b_{1g}$) and the second band in the 430–465 nm range is due to the $^1B_{1g}\leftarrow^1A_{1g}$ transition ($a_{1g}\rightarrow b_{1g}$), of square planar nickel(II) ions.[11,38,39] Cobalt(II) complexes (**13**) and (**19**) show three bands in the 435–450, 515–520 and 770–830 nm ranges, which are assigned to $^4T_{1g}(F)\rightarrow^4T_{1g}(P)$ (ν_3), $^4T_{1g}(F)\rightarrow^4A_{2g}(\nu_2)$ and $^4T_{1g}(F)\rightarrow^4T_{2g}(F)(\nu_1)$ transitions respectively, of high-spin octahedral cobalt(II) complexes.[25,40] The ν_2/ν_1 ratio for the complexes are in the 1.49–1.59 range (Table 3†), which are less than the usual range, indicating distorted octahedral cobalt(II) complexes. However, complex (**3**) shows bands at 490 and 550 nm (Table 3†) assigned to $^4T_{1g}\rightarrow^4T_{1g}(P)$ and $^4T_{1g}\rightarrow^4T_{2g}$ transitions, characteristic of a high-spin square planar cobalt(II) ion.[41] Manganese(II) complexes (**7**), (**9**) and (**24**) show bands in the 465–480, 540–560 and 635–650 nm ranges, assigned to $^6A_{1g}\rightarrow^4E_g$, $^6A_{1g}\rightarrow^4T_{2g}$ and $^6A_{1g}\rightarrow^4T_{1g}$, transitions, of octahedral geometry around the manganese(II) ion.[42] Chromium(III) complex (**21**) shows bands at 395, 445, 540 and 600 nm, the first band is assigned to a charge transfer transition and the last bands to $^4A_{2g}(F)\rightarrow^4T_{1g}(P)$, $^4A_{2g}(F)\rightarrow^4T_{1g}(F)$ and $^4A_{2g}\rightarrow^4T_{2g}(F)$ transitions, of an octahedral chromium(III) complex.[28,29] Copper(II) complexes (**2**), (**11**), and (**16**) show bands in the 450–460, 480–495 and 525–535 nm ranges (Table 3†), assigned to $^2B_{1g}\rightarrow^2B_{2g}$, $^2B_{1g}\rightarrow^2E_g$ and $^2B_{1g}\rightarrow^2A_1$ transitions respectively, of a square planar geometry[43,] and complex (**23**) shows bands at 445, 575 and 635 nm, assigned to $^2B_{1g}\rightarrow^2E_g$, $^2B_{1g}\rightarrow^2A_{1g}$ and $^2B_{1g}\rightarrow^2B_{1g}$ transitions, of an octahedral copper(II) complex.[43] The iron(III) complex (**20**) shows bands at 430, 460 and 660 nm. The first and second bands are assigned to charge transfer transitions while the last band is considered to arise from the $^6A_1\rightarrow^4T_1$ transition, from distorted octahedral geometry around the iron(III) ion.[44,45] Zinc(II) complexes (**5**), (**14**), (**18**), cadmium(II) complexes (**6**) and (**15**) and copper(I) complex (**22**) show bands (Table 3†), indicating intraligand transitions.

Thermal analyses

Thermal analysis (TGA and DTA) was carried out on complexes (**2**), (**11**), (**12**), (**13**), (**14**), (**17**), (**18**), (**19**) and (**22**) in the temperature range 25–800 °C. The results, detailed in Table 6† show a good agreement in the weight loss between the calculated and the found formulae. The thermal analysis showed that the complexes generally decomposed in several steps, the first step in the 50–130 °C range for all complexes corresponding to the dehydration process. The second step at 147 and 217 °C for complex (**19**) was assigned to elimination of coordinated water and another peak at 347 °C was due to elimination of coordinated (2OH). A second step in the 175–359 °C range for the complexes (**17**), (**18**), (**19**) and (**22**) was assigned to the elimination of chloride atom in the form of HCl. The peak in the 172–250 °C range for the complexes (**11**), (**12**), (**13**) and (**14**) corresponds to the elimination of coordinated nitrate in the form of HNO$_3$.[46,47] The third step in the 422–490 °C range was due to the complete decomposition with metal oxide formation.[46,47] The thermal decomposition of complex (**13**) can be represented as follows

$$[(HL)_2Co(NO_3)_2].2.5H_2O \xrightarrow{63\,°C} [(HL)_2Co(NO_3)_2].2H_2O + 1/2\,H_2O$$

$$[(HL)_2Co(NO_3)_2].2H_2O \xrightarrow{95\,°C} [(HL)_2Co(NO_3)_2] + 2H_2O$$

$$[(HL)_2Co(NO_3)_2] \xrightarrow{227\,°C} [(L)_2Co] + 2HNO_3$$

$$[(L)_2Co] \xrightarrow{461\,°C} CoO + \text{Volatile organic residue}$$

Antimicrobial studies

The antimicrobial screening data show that the compounds exhibit antimicrobial properties, the metal chelates exhibiting a greater inhibitory effect than the parent ligand, in comparison to tetracycline (as antibacterial agent) and amphotriciine (as antifungal agent). From the data obtained (Table 7†), it is observed that the inhibition zone area is much larger for metal complexes against the gram-positive bacteria (*Staphylococcus aureus*), gram-negative bacteria (*Escherichia coli*) and fungi (*Aspergillus flavus* and *Candida albicans*). The increased activity of the metal chelates can be explained on the basis of chelation theory.[48] It is know that chelation tends to make ligands act as more powerful and potent bactericidal agents and antifungal agents, thus killing more of the bacteria than the ligand. It is observed that, in a complex, the positive charge of the metal is partially shared with the donor atoms present in the ligand, and there may be π-electron delocalisation over the whole chelate.[48] This increases the lipophilic character of the metal chelate and favours its permeation through the lipoid layer of the bacterial membranes. Also, there are other factors which also increase the activity, such as solubility, conductivity and bond length between the metal and the ligand. The mode of action may involve the formation of a hydrogen bond through the azomethane nitrogen and oxygen atom with the active centres of the cell constituents, resulting in interference with the normal cell process. The variation in the effectiveness of different compounds against different organisms depend either on the impermeability of the cells of the microbes or the difference in ribosomes of microbial cells.[21] There is a marked increase in the bacterial activities of the ligand and complexes for gram positive bacteria, (*Staphylococcus aureus*): the order of activities are (**8**) = (**12**)>(**10**) = (**23**)>tetracycline = (**19**)>(**4**) = (**14**) = (**24**)>(**3**) = (**5**) = (**20**)>(**9**)>(**6**)>(**2**)>(**7**) = (**11**)>(**1**). For gram-negative bacteria, (*Escherichia coli*), the order of activities are (**20**) = (**24**) > tetracycline>(**10**) = (**23**)>(**19**)>(**4**) = (**12**)>(**8**)>(**5**) = (**6**) = (**14**)>(**3**) = (**11**)>(**2**) = (**7**)>(**9**)> (**1**). For *Asergillus flavus* we have (**24**)>(**9**) = (**23**)>(**8**) = (**14**) = (**20**)>(**7**) = (**12**) = (**19**)>(**10**)>(**5**)>(**6**) = (**11**) = amphotricine >(**2**) = (**3**) = (**4**)>(**1**). and for *Candida albicans* (**23**)>(**20**)>(**19**) = (**24**)>(**6**) = (**8**) = (**11**)> amphotricine = (**14**)>(**5**) = (**7**) = (**9**) = (**10**)>(**3**) = (**12**)>(**2**)>(**4**)>(**1**)

References

1 M.C. Rodriguez-Argüelles, M.B. Ferrari, F. Bisceglie, C. Pelizzi, G. Pelosi, S. Pinelli and M. Sassi, *J. Inorg. Biochem.*, 2004, **98**, 313.
2 D.F. Propp, *J. Hertocyclic Chem.*, 1984, **21**, 1641.
3 K. Anil Sen Gupta and A. Ateet Gupta, *Eur. J. Med. Chem. Ther.*, 1983, **18**, 181.
4 R.M. El-Bahnasawy, E. El-Shereafy and T.I. Kashar, *J. Thermal Analysis*, 1993, **39**, 65.
5 A.S. El-Tabl, F.A. El-Saied and A. Al-Hakimi, *Transition Met. Chem.*, 2007, **32**, 689.
6 A.I. Vogel, *A text book of quantitive inorganic analysis* 2nd edn, Longman, London, 1951.
7 H.A. Tang, L.F. Wang and R.D. Yang, *Transition Met. Chem.*, 2003, **28**, 395.
8 W.J Geary, *Coord. Chem. Rev.*, 1971, **7**, 81.
9 K.B. Gudasi, S.A. Patil, R.S. Vadvavi, R.V. Shenoy and M. Nethaji, *Transition Met. Chem.*, 2006, **31**, 586.
10 A.S. El-Tabl, *Transition Met. Chem.*, 1997, **22**, 400.
11 A.B.P. Lever *Inorganic Electronic spectroscopy* Elsevier publishing Company, New York, 1968, pp. 343-344.
12 H.M. El-Boraey and A.S. El-Tabl, *Polish J. Chem.*, 2003, **77**, 1759.
13 L. Mishra, A. Jha and A.K. Yadaw, *Transition Met. Chem.*, 1997, **22**, 406.

14 A.S. El-Tabl, K. El-Baradie and R.M. Issa, *J. Coord. Chem*., 2003, **56**, 1113.

15 S.K. Sengupta, O.P. Pandy, A. Rai and A. Sinha, *Spectrochim. Acta.* 2006, **A65**, 139.

16 W.H. Hegazy, *Monatsh. Chem*., 2001, **132**, 639.

17 L.K. Gupta, U. Banasal and S. Chandra *Spectrochim. Acta*, 2007, **A66**, 972.

18 S.D. Robenson and M.F. Uttly, *J. Chem. Soc*., 1973, 1912.

19 H.M. El-Tabl and F.A. El-Saied, *Synth. React. Inorg. Met.-Org. Chem.*, 2005, **35**, 243.

20 R.A. Lal and A. Kumar, *Indian J. Chem*., 1999, **38A**, 839.

21 Z.H. Abd. El-Wahab, M.M. Mashaly, A.A. Salman, B.A. El-Shetary and A.A. Faheim, *Spectrochim. Acta*, 2004, **60(A)**, 2861.

22 A.S El-Tabl and R.M. Issa, *J. Coord. Chem*., 2004, **57**, 509.

23 A.S. El-Tabl, *J. Chem. Res.**S**, 2002, 59.

24 A.K. El-Sawaf, D.X. West, F.A. El-Saied and R.M. El-Bahnasawy, *Syth. React. Inorg. Met. Org. Chem*., 1997, **27**, 1127.

25 J.K. Nag, S. Pal and C. Sinha, *Transition Met. Chem*., 2005, **30**, 523.

26 N. Raman, Y. Pitchaikani and A. Kulandaisamy, *Proc. Indian Acta. Sci.* (*Chem. Sci.*), 2001, **133**, 183.

27 B. Murukan and K. Mohanan, *Transition Met. Chem*., 2006, **31**, 441.

28 G.M. Abu El-Reash, K.M. Ibrahim and M.M. Bekheit, *Transition Met. Chem*., 1990, **15**, 148.

29 A.S. El-Tabl, *Transition Met. Chem*., 2002, **27**, 166.

30 S. Chandra and L.K. Gupta, *Spectrochim Acta*, 2004, **A60**, 2411.

31 M.C.R. Symons, T. Taiwo, A.M. Sargeson, M.M. Aly and A.S. El-Tabl, *Inorg. Chim. Acta*, 1996, **241**, 5.

32 I.M. Procter, B.J. Hathaway and P.N. Nicholls, *J. Chem. Soc.*, 1969, *A* 1678.

33 A.S El-Tabl, Ph.D. Thesis, Egypt 1993.

34 P.B. Sreeja, M.R.P. Kurup, A. Kishore and C. Jasmin, *Polyhedron*, 2004, **23**, 575.

35 N.V. Thakkar and S.Z. Bootwala, *Indian J. Chem*., 1995, **34A**, 370.

36 D.N. Sathyanarayana, *Electronic absorption spectroscopy and related techniques*, Orient Longman Lmited, Universities Press(India) Limited,2001.

37 A.S. El-Tabl and S.A. El-Enein, *J. Coord. Chem*., 2004, **57**, 281.

38 S. Mayadevi and K.K.M. Yusuff, *Synth. React. Inorg. Met-Org. Chem*., 1997, **27**, 319.

39 A. Cukurovali, I. Yalmaz and S. Kirbag, *Transition Met. Chem*., 2006, **31**, 207.

40 C.H. Krishna, C.M. Mahapatra and K.C. Dush, *J. Inorg. Nucl. Chem*., 1977, **39**, 1253.

41 A.K. Saxena, S. Saxena and A.K. Rai, *Synth. React. Inorg. Met.-Org. Chem* 1990, **20**, 21.

42 R.K. Parihari, R.K. Patel and R.N. Patel, *J. Ind. Chem. Soc*., 2000, **77**, 339.

43 A.S. El-Tabl, F.A. El-Saied and A. El-Hakimi, *J. Coord. Chem*., 2008, **61**, 2380.

44 S.A. Sallam, A.S. Orabi, B.A. El-Shetary and A. Lentz, *Transition Met. Chem*., 2002, **27**, 447.

45 N.K. Singh and S.B. Singh, *Transition Met. Chem*., 2001, **26**, 487.

46 A.S El-Tabl, R.M. Issa and M.A. Morsi, *Transition Met. Chem*., 2004, **29**, 543.

47 A.S. El-Tabl and S.M. Imam, *Transition Met. Chem.* 1997, **22**, 259.

48 S.K. Sengupta, O.P. Pandy, B.K. Srivastava and V.K. Sherma, *Transition Met. Chem*., 1998, **23**(4), 349.